Chemical Research in Toxicology

MARCH/APRIL 1989
VOLUME 2, NUMBER 2

Perspective

Photochemistry of the Psoralens

John E. Hearst

College of Chemistry, University of California, Berkeley, California 94720

Received March 10, 1989

Introduction

Psoralen is a three-ring heterocyclic compound with the structure

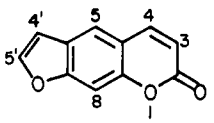

Psoralen-containing plants have been used since the beginnings of written history in the cures of various skin disorders. This is not terribly surprising, considering the large numbers of plants that contain psoralens. Identification of the active plants in these cures and recognition of the need for the use of sunlight actually occurred much later, perhaps between 300 B.C. and 600 A.D. (*1*). The physiological activity of this family of compounds was apparently described in old Arabic literature (1400 B.C.), where reference was made to the use of fruits of *Ammi majus* as a remedy for leukoderma (*2*). The purified compounds are used in the treatment of psoriasis and vitiligo (*2*, *3*). When psoralens are administered, either topically to the skin or orally, they sensitize the skin to near-ultraviolet light, inducing tanning and sunburn. Such treatment results in remission of the symptoms of psoriasis.

The suggestion that psoralens photoreact with DNA and result in the cross-linkage of the two strands of the DNA helix first appeared in 1971 (*4*, *5*). The synthetic organic chemistry resulting in modified psoralens has been extensive (*6*). The most commonly used psoralens are shown in Figure 1. The greater solubilities in water provided by the hydroxymethyl substitution in HMT and the aminomethyl substitution in AMT are major factors in the greater efficiency of the photochemistry using these compounds relative to the natural products. Isaacs et al. (*6*) proved that RNA helices are also cross-linked by psoralen photochemistry.

The mechanism of the photoaddition of a psoralen to a nucleic acid helix involves several steps. The initial step is the intercalation of the psoralen into the nucleic acid helix in a dark reaction, reaction 1. While it is likely that this intercalation is somewhat sequence specific, this has not yet been demonstrated. When an intercalated psoralen absorbs a photon of wavelength between 300 and 400 nm, it is sensitized to react by cycloaddition at either the 3,4 double bond of the pyrone ring or the 4′,5′ double bond of the furan ring with the 5,6 double bond of an adjacent pyrimidine, reaction 2. The second cycloaddition, to the opposite nucleic strand from the position of the first adduct, can only form if two conditions are met. First, the monoadduct formed in reaction 2 must be a furan-side monoadduct (cycloaddition in reaction 2 must have occurred at the 4′,5′ double bond of the psoralen). Only in this case is the remaining adduct a coumarin derivative which can still absorb a photon of wavelength between 300 and 380 nm, making reaction 3 possible. Second, a pyrimidine has to be adjacent to the psoralen monoadduct on the opposite strand. Thus, for cross-link to form, the original intercalation had to occur in either a 5′ purine–pyrimidine 3′ site or in a 5′ pyrimidine–purine 3′ site in the helix. Johnson et al. (*7*) proved that a time delay of approximately 1 μs must occur between the absorption of the photon leading to the monoaddition of the psoralen to the first strand and the absorption of the second photon leading to efficient formation of cross-link to the opposite strand. This time delay has been associated with a major conformational change in the modified helix prior to cross-link formation. Figure 2 provides a schematic representation of the reaction mechanism which represents this conformational change as a kink in the helix.

0893-228x/89/2702-0069$01.50/0

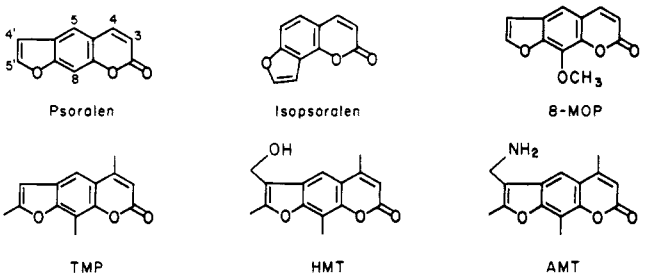

Figure 1. Various psoralens—psoralen, isopsoralen (angelicin), 8-methoxypsoralen (8-MOP), 4,5′,8-trimethylsporalen (TMP) (trioxsalen), 4′-(hydroxymethyl)-4,5′,8-trimethylpsoralen (HMT), and 4′-(aminomethyl)-4,5′,8-trimethylpsoralen (AMT).

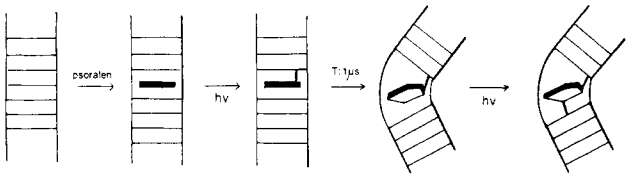

Figure 2. Mechanism of the photoreactions of psoralens with the DNA helix. The first step is a thermal reaction involving the intercalation of the psoralen in the helix. The second step is cyclobutane addition after the absorption of a photon. The third step is a major conformational change in the helix at the position of the psoralen monoadduct. The final step is the formation of the second cyclobutane ring upon absorption of a second photon, thus creating a covalent cross-link between the two strands of the DNA helix.

Several specificities intrinsic to the photochemistry of the psoralens with DNA and RNA have been demonstrated. The stereochemistry of the products is dictated by the DNA and RNA helices and will be discussed in detail in the next section. Piette et al. (*8*) have shown that in DNA 5′TpA3′ sites are far more photoreactive than the 5′ApT3′ site in model oligonucleotide DNA helices. Tessman et al. (*9*) have demonstrated a similar bias in reactivity in DNA by observing that the stereochemical product expected from the first of these sequences is 3–14 times more prevalent than the opposite product, depending on the detailed conditions used during the photochemical reaction and the extent of the reaction of the DNA with psoralen. These studies clearly prove that the most reactive sites in DNA are thymines which react with a psoralen on the 3′ side of the thymine. Nevertheless, if the photochemical reaction is pushed to near saturation of the DNA, addition densities higher than 1 psoralen adduct per 5 base pairs can be obtained (*6*). Such numbers suggest that most pyrimidines in nucleic acid helices are photoreactive, but the rates of reactivity are base and sequence dependent. It is clear that thymines and uracils are more reactive than cytosines. Another interesting specificity revealed by Kanne et al. (*10*) relates to the probability of furan-side monoaddition versus pyrone-side monoaddition to DNA. Kanne et al. (*10*) have shown that psoralen derivatives with a 4-methyl substitution show an overwhelming preference (98%) for addition to the furan double bond, while compounds with a hydrogen at the 4-carbon show nearly 20% monoaddition to the pyrone double bond.

Structural Characterization of the Adducts

The photoadducts of HMT, TMP, and 8-MOP to DNA have been examined after isolation of the photoadducted mononucleosides by extensive enzymatic hydrolysis of photoreacted DNA. The various products were isolated on reverse-phase HPLC, a process that was greatly assisted by the availability of tritium-labeled psoralen derivatives

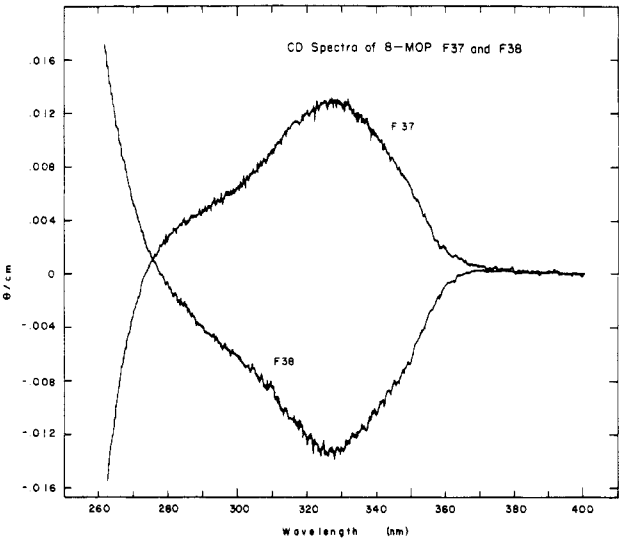

Figure 3. The circular dichroism of the two cys-syn furan-side monoadducts between 8-MOP and thymidine. These two hydrolysis products have opposite and equal circular dichroism spectra, as expected for a pair of enantiomers, since the deoxyribose moiety influences the overall molar ellipticity of each diastereomer to a very small degree. Which of the two possible cis-syn diastereomers forms is determined by whether the psoralen is on the 3′ or the 5′ side of the thymidine with which it reacts in the helix.

(*11*). In general, three nucleoside–psoralen monoaddition products have been isolated and characterized, corresponding to three deoxythymidine–psoralen adducts. In some cases two minor deoxyuridine–psoralen adducts derived from an initially formed deoxycytidine adduct by hydrolytic deamination were found. The major products are two diastereomeric thymidine adducts formed by cycloaddition between the 5,6 double bond of the thymine and the 4′,5′ (furan) double bond of the psoralen. The third thymidine adduct has been shown to be the cycloaddition product between the 5,6 double bond of the thymine and the 3,4 (pyrone) double bond of the psoralen. The pyrone adduct represented 20% of the covalently bound 8-MOP to DNA but less that 3% of the covalently bound TMP (*12–14*). The two prominent diastereomers have equal but opposite sign circular dichroism spectra (Figure 3), suggesting that they are identical in structure except that in one case cycloaddition has occurred on the 3′ side of the thymidine on the phosphodiester chain while in the other case cycloaddition has occurred on the 5′ side of the thymidine.

These three products are a small fraction of the cycloaddition products that are possible. Figure 4 shows some of these potential stereoisomers. The fact that only the cis-syn adducts are isolated from DNA indicates that the DNA helix itself has a structural role in determining the addition products formed. The unambiguous assignment of the configuration and stereochemistry of the addition products was first achieved by NMR. The assignment of all the protons in these nucleoside monoadducts is straightforward (*12–16*), establishing the chemistry as cycloaddition chemistry and positioning the reactive double bonds. The stereochemistry of the products has been established by NOE experiments. A similar analysis has been possible on the isolated thymidine–psoralen–thymidine cross-link. Figure 5 shows the NOE spectra on the TMP cross-link, establishing that both cyclobutane stereochemistries are cis-syn.

A racemic mixture of the furan-side monoadduct between 8-MOP and thymine has been isolated from DNA and the purified racemate crystallized for X-ray crystal-

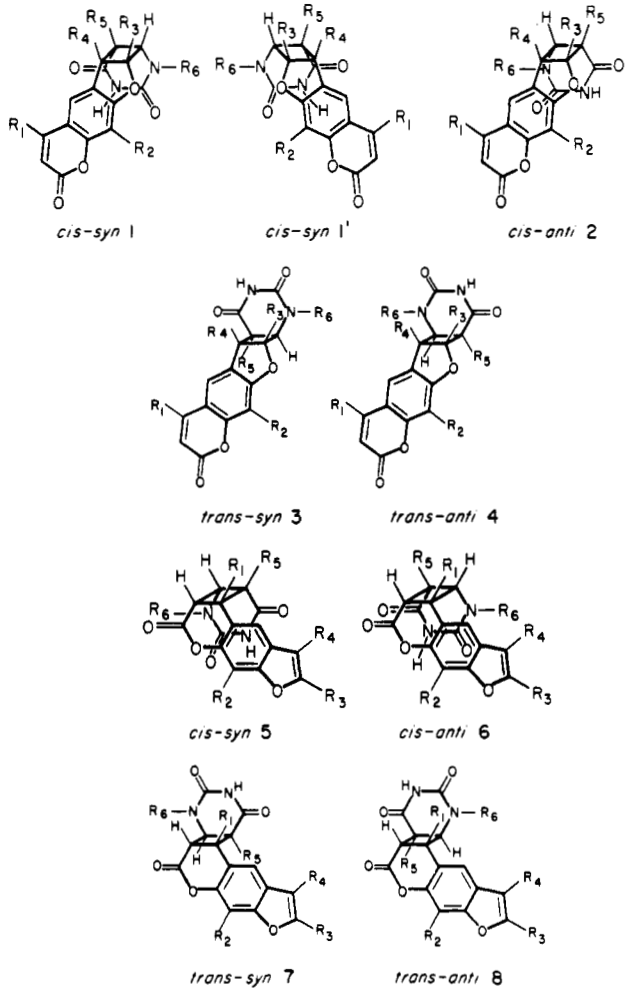

Figure 4. Various possible cycloaddition products between the psoralens and thymidine. 1 and 1′ are the near enantiomer pair discussed in Figure 3. Such a pair exists for each of the remaining adducts shown in this figure. 1–4 are furan-side monoadducts. 5–8 are pyrone-side monoadducts.

lographic analysis. The unit cell contained six monoadducts, thymine–8-MOP, three of each enantiomer. This structure verified the assignment of the adduct as a cis-syn cyclobutane adduct. The crystal structure indicated that both the thymine ring and the psoralen ring remain planar in the photoadduct and that the three nonequivalent compounds in the unit cell showed angles of 44.1°, 50.6°, and 53.5° between the two planes, indicating considerable flexibility in the cyclobutane bridge (*17*, *18*). On the assumption that the angles between the rings at the pyrone end of the psoralen in the DNA cross-link are similar to those determined in this crystal structure, the psoralen cross-link has been predicted to create a kink in the DNA backbone.

The two-dimensional NMR analysis has been completed on the AMT cross-link of the oligonucleotide d-GGGTACCC. Figure 6 shows the standard sequential connectivities in (A) for the unmodified oligonucleotide helix and in (B) for each of the independent four half-strands which are separated by the drug in the cross-linked oligonucleotide. By use of the methods of distance geometry, a 3D structure has been proposed and is shown as a stereopair in Figure 7. The structure includes a kink in the DNA helix backbone as well as clear asymmetry in the base-pairing stability in the region adjacent to the cross-link (*19*). This asymmetry is also clearly indicated by the temperature dependences of the imino resonances, which are shown in Figures 8 and 9. At the present time

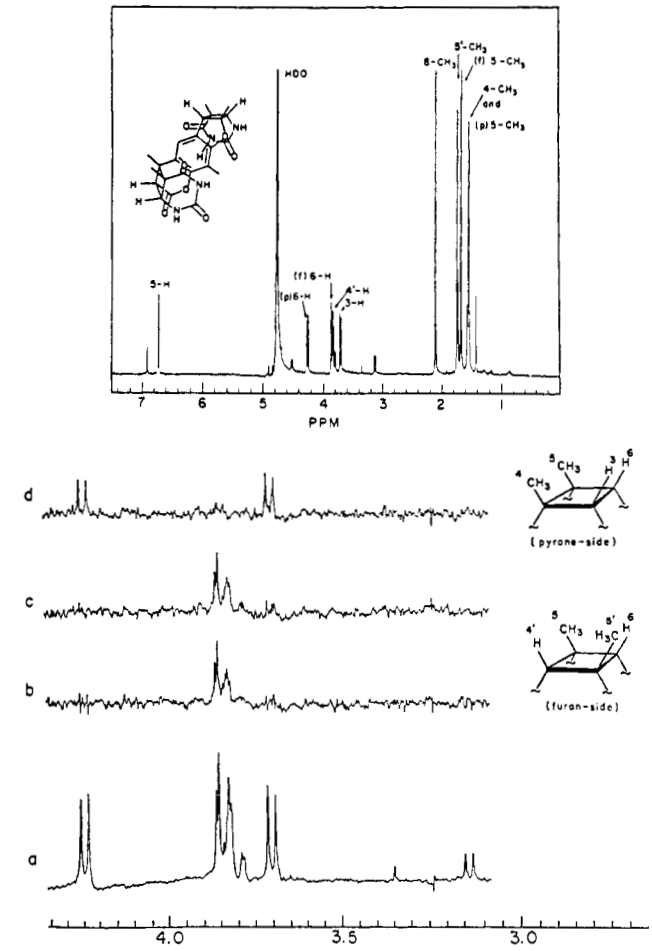

Figure 5. (Above) The 360-MHz proton NMR spectrum of a thymine–trioxsalen–thymine cross-link in D_2O. (Below) Nuclear Overhauser enhancements for the thymine–trioxsalen–thymine cross-link: (a) 3.5–4.5-ppm region of the proton NMR spectrum; (b) difference spectrum between sample irradiated in the 5′-CH_3 resonance (1.76 ppm) and (a), demonstrating proximity to the C6-H (3.87 ppm) and to the C4′-H (3.87 ppm) at the furan-side cyclobutane ring; (c) difference spectrum between sample irradiated in the 5-CH_3 (dT) resonance (1.66 ppm) and (a), demonstrating proximity to the C6-H (3.87 ppm) and to the C4′-H (3.83 ppm) at the furan-side cyclobutane ring; (d) difference spectrum between sample irradiated in the 4-CH_3 and 5-CH_3 (dT) (1.54 ppm) and (a), demonstrating proximities to C6-H (4.25 ppm) and to C3-H (3.87 ppm) at the pyrone-side cyclobutane ring.

it is uncertain if other structures might also be consistent with the 2D NMR data.

Application to Structure Determination

As natural products, the psoralens have evolved with remarkable abilities to penetrate both cells and virus particles. This fact was first demonstrated with the photoreaction of trioxsalen with isolated *Drosophila melanogaster* and mouse liver interphase nuclei (*20*, *21*) and with mouse L cells in vivo (*22*). The DNA isolated from these reactions was spread under denaturing conditions for electron microscopic examination. The cross-links were observed to occur in a pattern with a regular repeat of approximately 200 base pairs. This pattern was proven to be the result of a high reactivity of the chromatin DNA in the interbead or linker regions of chromatin by correlating the positions of the cross-links with the regions of micrococcal nuclease sensitivity (*23*).

There is a large literature reporting the photoreaction of psoralens with viruses. Much of this activity is directed at virus inactivation and vaccine production. Examples include vesicular stomatitis virus, SV-40 virus, polio 1 and

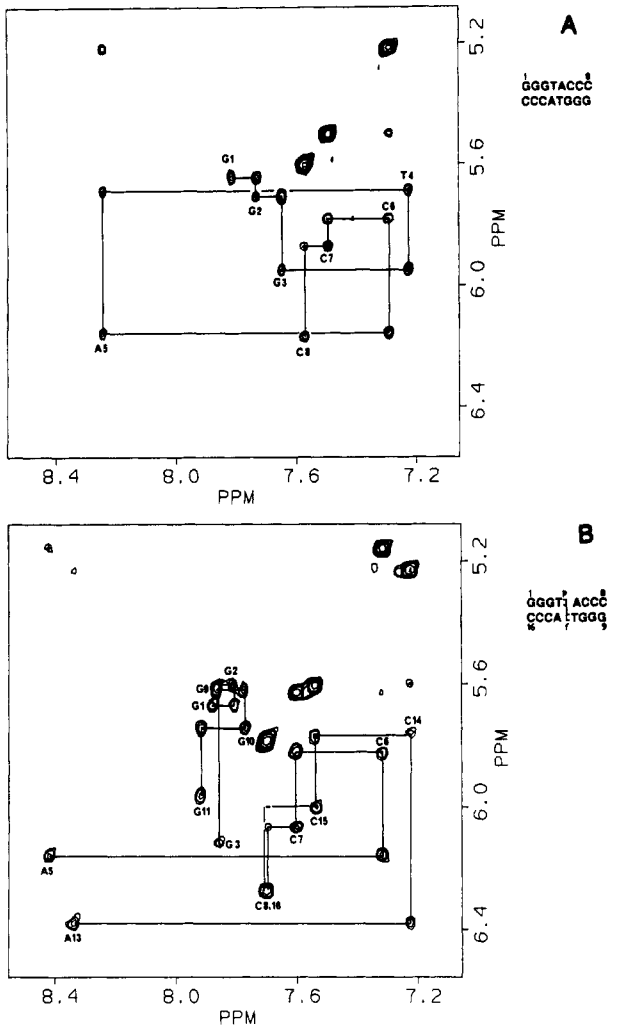

Figure 6. Expansions of the 2D NOE spectrum of d-GGGTACCC showing the cross-peaks of the aromatic proton to H1′ of the same nucleotide (numbered peaks) and to the H1′ of the sugar of the base on the 5′ side (connected with solid lines). (A) Unmodified octamer possessing a center of symmetry with all the protons sequentially assigned. (B) Cross-linked oligomer where the residues on either side of the drug are no longer equivalent. T4 is linked to the pyrone side ("p") and T12 is linked to the furan side ("f") of the 4′-(aminomethyl)-4,5′,8-trimethylpsoralen.

2, herpes simplex 1 and 2, influenza, vaccinia, blue tongue virus, murine sarcoma, canine hepatitis, western equine encephalitis, and the AIDS virus HIV (*24*). The photo-cross-linking reaction has been applied to the investigation of DNA structure in virus particles. The best example relates to the fd phage, which contains a circular single-stranded DNA genome of 6408 bases. The origin of DNA replication is known from sequencing studies to contain a complex of four hairpins which when cross-linked is readily visualized by electron microscopy. The phage particle is a long cylindrical filament with the DNA at its center. The object of the cross-linking experiment is to establish if the circular DNA is oriented in a specific way in the phage particle or if it is randomly permuted. Cross-linkage established that the origin complex is located at the end of the filamentous phage.

16S rRNA has been extensively studied by psoralen photo-cross-linkage. A cross-linkage map was first generated by using electron microscopy. These maps were generated both for the isolated 16S rRNA in vitro and for the same rRNA in the 30S subunit of the ribosome. It was concluded, to the sensitivity of this assay, that RNA has equivalent regions of secondary structure in both molecules (*25*, *26*). These mapping procedures are now performed for sequence resolution. These studies have provided tentative evidence for conformational switches in the rRNA cycle. Figure 10 presents a model showing the positions of the observed psoralen cross-links superimposed on the phylogenetic secondary structure map of Noller and Woese (*27*). In addition, sites hypothesized to be associated with the initiation of translation or mRNA binding, and with tRNA binding, are shown (*28*).

Hybridization Dynamics

Site-specific placement of a furan-side psoralen monoadduct in synthetic oligonucleotides is possible because of the greater photoreactivity of 5′TpA3′ sites than any other potential photoaddition sites. Synthetic oligonucleotides containing only one such site are added to a complementary strand of different length (to facilitate electrophoretic gel separation), and the mixture plus a psoralen is irradiated at 390 nm. The monoadducted oligonucleotide is then isolated and purified by gel electrophoresis or high-performance liquid chromatography (*8*, *29*). These monoadducted oligonucleotides may now be used as hybridization probes which can be irreversibly bonded to their target sequence by near-ultraviolet light. Hearst (*30*) has presented a theory which demonstrates that the optimal condition for hybridization are at the melting temperature of the oligonucleotide from its target or at the point where half of the target is covered and half is free. This point provides maximum discrimination with respect to the partial homologies that may occur between probe and target. In addition, high probe concentration favors rapid attainment of equilibrium but also reduces discrimination. In general, it is concluded that optimal hybridization conditions occur near a probe concentration of 10^{-8} M, where the half-life for the hybridization reaction is 43 s. While these conditions are readily achievable, in order to separate unreacted probe from target in a hybridization reaction, a wash step is essential. For conditions favoring such rapid reaction, a rapid fixation step is essential, and it is in this context that the photo-cross-linkable probe proves useful. The hybridization of an oligonucleotide probe to a high molecular weight single-stranded target is complex for two additional reasons. First, the single-stranded target invariably contains considerable secondary structure which competes for the target sequence, and second, the complementary long strand can hybridize to the target, displacing the probe. These variables have been experimentally examined in detail (*31*, *32*), and the phenomenon of photochemical "pumping" has been described. Figure 11 provides evidence for the effects discussed above. For the reaction of small probes with large targets, the photo-cross-linkable probes provide a unique tool for the study of the kinetics and equilibria of importance to the process. For such a study to be meaningful, the monoadduct should modify the interaction of probe with target as little as possible. Shi and Hearst (*33*) have demonstrated this to be the case for monoadducts of HMT in 5′TpA3′ sites. In addition, the use of tetraalkylammonium salts in the hybridization solution can be used to minimize the base compositional dependence of the thermodynamic interactions, making the hybridization dependent only on the length of the base-pairing interaction (*34*, *35*).

DNA–Protein Interactions

Piette and Hearst (*36*) have used a double-stranded circular DNA which was photoreacted with HMT as a substrate for nick-translation with *Escherichia coli* DNA polymerase I holoenzyme. The template DNA had a sin-

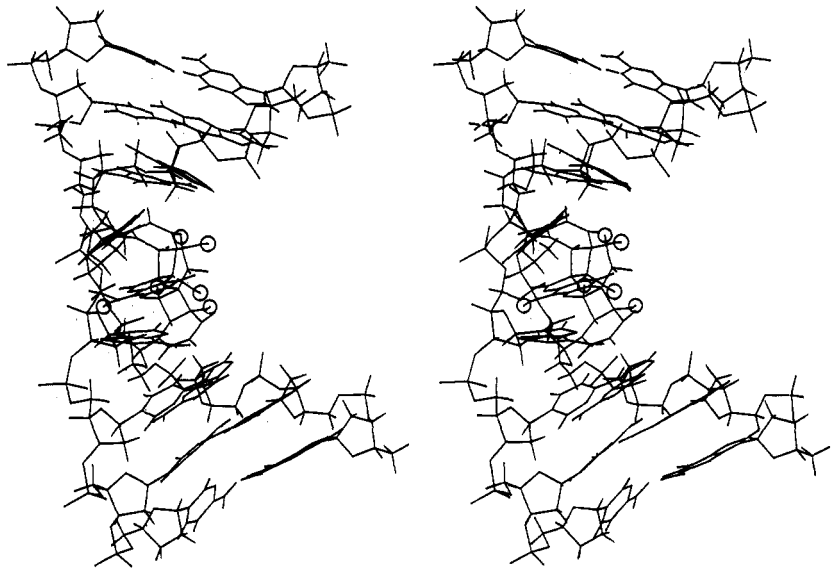

Figure 7. Stereo picture of the NMR-derived model for DNA octamer duplex cross-linked with (aminomethyl)trioxsalen. All of the methyl groups and the amino group of AMT are indicated by circles.

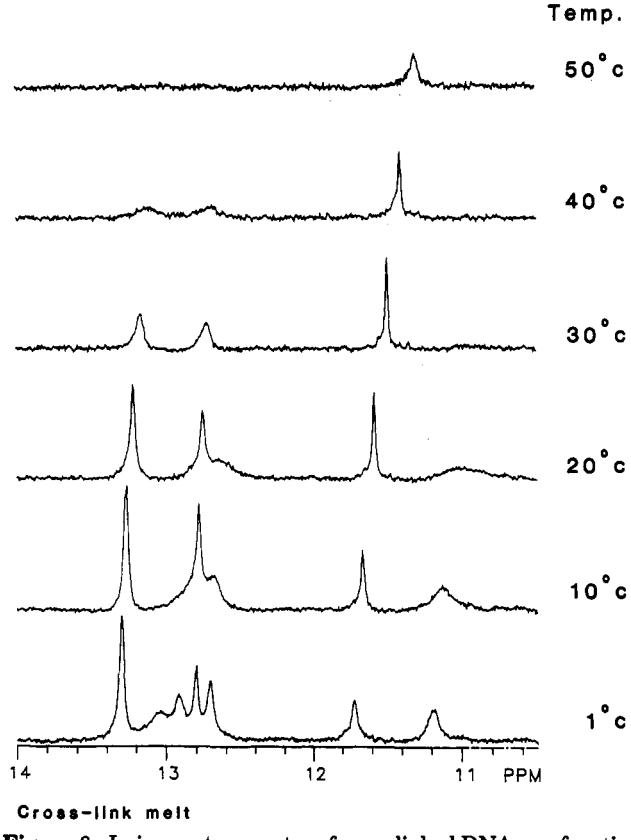

Figure 8. Imino proton spectra of cross-linked DNA as a function of temperature.

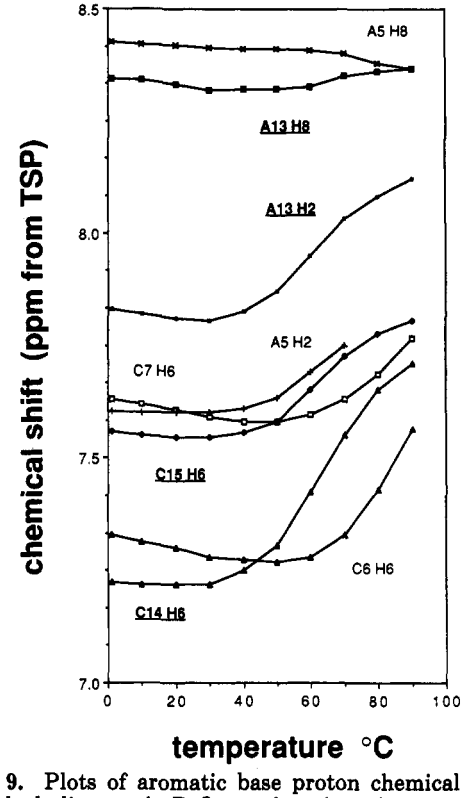

Figure 9. Plots of aromatic base proton chemical shifts of cross-linked oligomer in D_2O as a function of temperature.

gle-stranded nick at a specific site so that the positions of pauses and stops in the nick-translation process could be mapped to sequence resolution. They showed that psoralen monoadducts on the template strand resulted in kinetic pauses in DNA nick translation but that incorporation of adenine opposite the monoadducted thymine still occurred. This suggests that a monoadducted base may still base pair to its complement strand and that such a monoadducted thymine can code for its complementary base during DNA replication with high fidelity. These data indicate that it is the psoralen cross-link and not the monoadduct that is responsible for the lethal effects of psoralen photochemistry in *E. coli*. In fact, Chanet et al. (*37*) have shown that, in yeast, psoralen monoadducts are retained through several cell divisions with no evidence of mutagenesis, suggesting that such monoadducted DNA may properly code for its complementary strand in vivo. Physical evidence for the base-pairing capacity of the thymine monoadduct in the DNA helix has been obtained by the two-dimensional NMR study of Tomic et al. (*19*).

By site-specific placement of psoralens into oligonucleotides, it has been possible to generate specific substrates for a number of interesting enzymic processes. Included in this list have been *E. coli* RNA polymerase (*38*), T7 RNA polymerase (*39*), uvrABC excinuclease (*40*), and recA (*41*). An in vitro model for DNA cross-link repair in *E. coli* has been developed by using the last two of these examples. Figure 12 demonstrates the sequential steps in this modeled repair process (*40*). Cheng et al. (*41*) have studied the hybridization between a single-stranded mo-

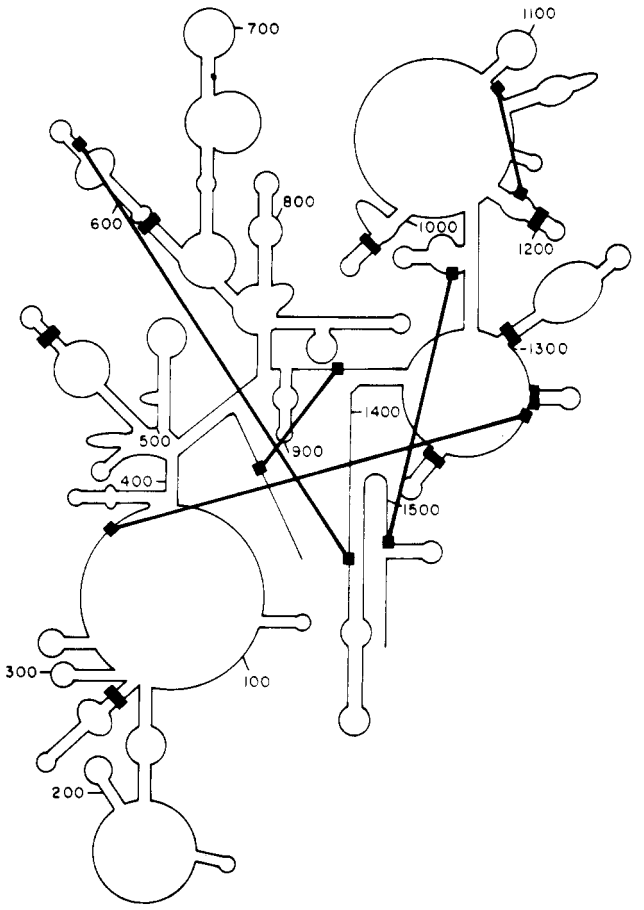

Figure 10. The locations of 13 HMT cross-links in 16S ribosomal RNA superimposed over the skeleton of the secondary structure model presented by Noller and Woese (*27*).

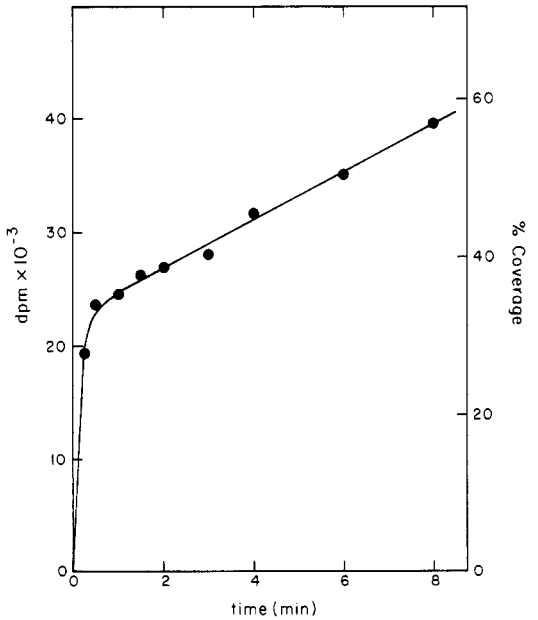

Figure 11. Continuous photochemical pumping of the hybridization equilibrium between a HMT-monoadducted 25-mer oligonucleotide and single-stranded M-13 mp19 target DNA. Annealing and photofixation were carried out at 45 °C in 35% formamide. Notice that 30% of the target reacts in less than a minute, but reaction of the remaining target evidently requires a slow conformational change which makes the target sequence available to the probe.

noadducted oligonucleotide and its complementary sequence within a duplex DNA molecule, a reaction catalyzed by the recA protein of *E. coli*. The fact that the

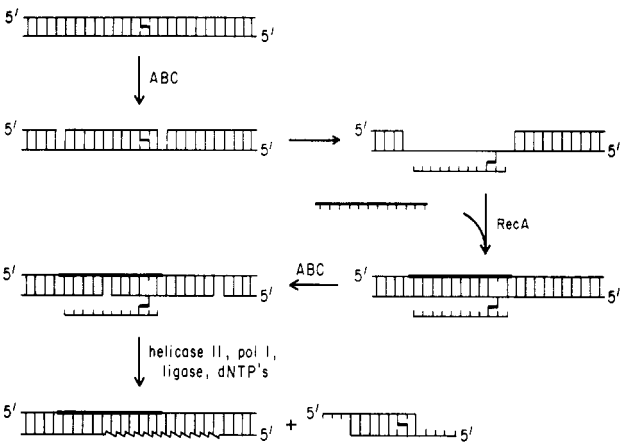

Figure 12. The repair pathway for DNA–psoralen cross-links suggested by in vitro experiments with site-specifically modified oligonucleotide substrates, the *E. coli* excinuclease complex uvrABC, recA, DNA polymerase, and ligase.

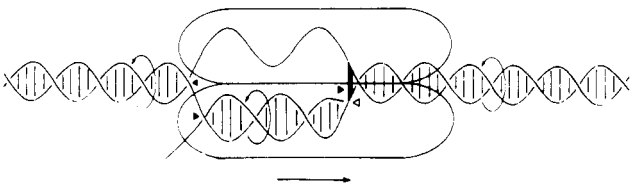

Figure 13. A model for the *E. coli* RNA polymerase transcription elongation complex. The horizontal arrow indicates the direction of RNA synthesis. The curved arrows indicate the unwinding and rewinding of DNA of DNA–RNA helix by the polymerase. The filled triangles denote the hypothetical unwindase and rewindase centers of the enzyme. The open triangle denotes the catalytic site of the polymerase, which is very close to the leading unwindase site. The vertical bar indicates the site of the psoralen cross-link which was used to arrest RNA polymerase elongation. The footprint of the polymerase on the DNA is indicated by the length of the two lobes of the enzyme relative to the turns of the DNA helix.

three-strand complex that occurs in this system comprised of the oligonucleotide covered with recA protein and the DNA target duplex can be photochemically fixed has been interpreted as a clear indication that base pairing is the structural interaction between the oligonucleotide and its complementary target.

A model for the ternary elongation complex between *E. coli* RNA polymerase, the DNA template, and the newly synthesized RNA molecule has been formulated from footprinting studies on such a complex arrested at a psoralen cross-link. The results of this study are summarized in Figure 13 (*38*).

References

(1) Scheel, L. D. (1967) In *Biochemistry of Some Foodborne Microbial Toxins* (Mateles, R. I., and Wogan, G. N., Eds.) p 109, MIT Press, Cambridge, MA.
(2) Pathak, M. A., and Fitzpatrick, T. B. (1959) Relationship of Molecular Configuration to the Activity of Furocoumarins which Increase the Cutaneous Responses Following Long Wave Ultraviolet Radiation. *J. Invest. Dermatol.* **32**, 255–262.
(3) Scott, D. R., Pathak, M. A., and Moh, G. R. (1976) Molecular and Genetic Basis of Furocoumarin Reactions. *Mutat. Res.* **39**, 29–74.
(4) Cole, R. S. (1971) Psoralen Monoadducts and Interstrand Cross-links in DNA. *Biochim. Biophys. Acta* **254**, 30–39.
(5) Dall'acqua, F., Marciani, S., Ciavatta, L., and Rodighiero, G. (1971) Formation of Inter-Strand Cross-Linkings in the Photoreactions between Furocoumarins and DNA. *Z. Naturforsch.* **B26**, 561–569.
(6) Isaacs, S. T., Shen, C.-K. J., Hearst, J. E., and Rapoport, H. (1977) Synthesis and Characterization of New Psoralen Deriva-

tives with Superior Photoreactivity with DNA and RNA. *Biochemistry* **16**, 1058–1064.
(7) Johnston, B. H., Kung, A. H., Moore, C. B., and Hearst, J. E. (1981) Kinetics of Formation of Deoxyribonucleic Acid Cross-Links by 4′-(Aminomethyl)-4,5′,8-trimethylpsoralen. *J. Am. Chem. Soc.* **20**, 735–738.
(8) Gamper, H., Piette, J., and Hearst, J. E. (1984) Efficient Formation of a Crosslinkable HMT Monoadduct at the KpnI Recognition Site. *Photochem. Photobiol.* **40**, 29–34.
(9) Tessman, J. W., Isaacs, S. T., and Hearst, J. E. (1985) Photochemistry of the Furan-Side 8-Methoxypsoralen–Thymidine Monoadduct Inside the DNA Helix. Conversion to Diadduct and to Pyrone-Side Monoadduct. *Biochemistry* **24**, 1669–1676.
(10) Kanne, D., Rapoport, H., and Hearst, J. E. (1984) 8-Methoxypsoralen–Nucleic Acid Photoreaction. Effect of Methyl Substitution on Pyrone vs. Furan Photoaddition. *J. Med. Chem.* **27**, 531–534.
(11) Isaacs, S. T., Rapoport, H., and Hearst, J. E. (1982) Synthesis of Deuterium and Tritium Labeled Psoralens. *J. Labelled Compd. Radiopharm.* **19**, 345–356.
(12) Straub, K., Kanne, D., Hearst, J. E., and Rapoport, H. (1981) Isolation and Characterization of Pyrimidine–Psoralen Photoadducts from DNA. *J. Am. Chem. Soc.* **103**, 2347–2355.
(13) Kanne, D., Straub, K., Rapoport, H., and Hearst, J. E. (1982) Psoralen–Deoxyribonucleic Acid Photoreaction. Characterization of the Monoaddition Products from 8-Methoxypsoralen and 4,5′,8-Trimethylpsoralen. *Biochemistry* **21**, 861–871.
(14) Kanne, D., Straub, K., Hearst, J. E., and Rapoport, H. (1982) Isolation and Characterization of Pyrimidine–Psoralen–Pyrimidine Photoadducts from DNA. *J. Am. Chem. Soc.* **104**, 6754–6764.
(15) Cimino, G. D., Gamper, H. B., Isaacs, S. T., Hearst, J. E. (1985) Psoralens as Photoactive Probes of Nucleic Acid Structure and Function: Organic Chemistry, Photochemistry, and Biochemistry. *Annu. Rev. Biochem.* **54**, 1151–1193.
(16) Hearst, J. E., Isaacs, S. T., Kanne, D., Rapoport, H., and Straub, K. (1984) The Reaction of the Psoralens with Deoxyribonucleic Acid. *Q. Rev. Biophys.* **17**, 1–44.
(17) Peckler, S., Graves, B., Kanne, D., Rapoport, H., Hearst J. E., and Kim, S.-H. (1982) Structure of a Psoralen–Thymine Monoadduct Formed in Photoreaction with DNA. *J. Mol. Biol.* **162**, 157–172.
(18) Kim, S.-H., Peckler, S., Graves, B., Kanne, D., Rapoport, H., and Hearst, J. E. (1983) Sharp Kink of DNA at Psoralen-crosslink Site Deduced from Crystal Structure of Psoralen–Thymine Monoadduct. *Cold Spring Harbor Symp. Quant. Biol.* **47**, 361–365.
(19) Tomic, M. T., Wemmer, D. E., and Kim, S.-H., (1988) Structure of a Psoralen Cross-Linked DNA in Solution Determined by Two-Dimensional NMR. *Science* **238**, 1722–1725.
(20) Hanson, C. V., Shen, C.-K. J., and Hearst, J. E. (1976) Cross-Linking of DNA in situ as a Probe for Chromatin Structure. *Science* **193**, 62–64.
(21) Cech, T., and Pardue, M. L. (1977) *Crosslinking* of DNA with Trimethylpsoralen is a Probe for Chromatin Structure. *Cell* **11**, 631–640.
(22) Cech, T., Potter, D., and Pardue, M. L. (1978) Chromatin Structure in Living Cells. *Cold Spring Harbor Symp. Quant. Biol.* **42**, 191–198.
(23) Weisehahn, G. P., Hyde, J. E., and Hearst, J. E. (1977) The Photoaddition of Trimethylpsoralen to Drosophila melanogaster Nuclei: A Probe for Chromatin Substructre. *Biochemistry* **16**, 925–932.
(24) Hanson, C. V. (1983) Inactivation of Viruses for Use as Vaccines and Immunodiagnostic Reagents, Medical Virology II (de la Maza, L. M., and Peterson, E. M., Eds.) pp 45–79, Elsevier, New York.
(25) Wollenzien, P., Hearst, J. E., Thammana, P., and Cantor, C. R. (1979) Base-pairing between Distant Regions of the Escherichia coli 16S Ribosomal RNA in Solution. *J. Mol. Biol.* **135**, 255–269.
(26) Thammana, P., Cantor, C. R., Wollenzien, P. L., and Hearst, J. E. (1979) Crosslinking Studies on the Organization of the 16S Ribosomal RNA within the 30 S Escherichia coli Ribosomal Subunit. *J. Mol. Biol.* **135**, 271–283.
(27) Noller, H. F., and Woese, C. R. (1981) Secondary Structure of 16S Ribosomal RNA. *Science* **212**, 403–411.
(28) Thompson, J. F., and Hearst, J. E. (1983) Structure of E. Coli 16S RNA Elucidated by Psoralen Crosslinking. *Cell* **32**, 1355–1365.
(29) Shi, Y., and Hearst, J. E. (1987) Wavelength Dependence for the Photoreactions of DNA–Psoralen Monoadducts. 1. Photoreversal of Monoadducts. 2. Photo-Cross-Linking of Monoadducts. *Biochemistry* **26**, 3786–3798.
(30) Hearst, J. E. (1987) Background Hybridization Associated with the Use of Photocrosslinkable Oligonucleotide Hybridization Probes for the Identification of Unique Sequences in the Human Genome. *Photobiochem. Photobiophys., Suppl.*, 23–32.
(31) Gamper, H. B., Cimino, G. D., Isaacs, S. T., Ferguson, M., and Hearst, J. E. (1986) Reverse Southern Hybridization. *Nucleic Acids Res.* **14**, 9943–9954.
(32) Gamper, H. B., Cimino, G. D., and Hearst, J. E. (1987) Solution Hybridization of Crosslinkable DNA Oligonucleotides to M13DNA: Effect of Secondary Structure on Hybridization Kinetics and Equilibria. *J. Mol. Biol.* **197**, 349–362.
(33) Shi, Y., and Hearst, J. E. (1986) Thermostability of Double-Stranded Deoxyribonucleic Acids: The Effects of Covalent additions of a Psoralen. *Biochemistry* **25**, 5895–5902.
(34) Shapiro, J. T., Stannard, B. S., and Felsenfeld, G. (1969) The Binding of Small Cations to Deoxyribonucleic Acid. Nucleotide Specificity. *Biochemistry* **8**, 3233–3241.
(35) Melchior, W. B., Jr., and von Hippel, P. H. (1973) Alteration of the Relative Stability of dA·dT and dG·dC Base Pairs in DNA. *Proc. Natl. Acad. Sci. U.S.A.* **70**, 298–302.
(36) Piette, J. G., and Hearst, J. E. (1983) Termination Sites of the in vitro Nick-Translation Reaction on DNA that had Photoreacted with Psoralen. *Proc. Natl. Acad. Sci. U.S.A.* **80**, 5540–5544.
(37) Chanet, R., Cassier, C., Magana-Schwenke, N., and Moustacchi, E. (1984) Fate of Photoinduced 8-Methoxypsoralen Monoadducts in Yeast. Evidence for Bypass of these Lesions in the Absence of Excision. *Mutat. Res.* **112**, 201–214.
(38) Shi, Y., Gamper, H., Van Houten, B., and Hearst, J. E. (1988) Interaction of E. coli RNA Polymerase with DNA in an Elongation Complex Arrested at a Site Specific Cross-link Site. *J. Mol. Biol.* **199**, 277–293.
(39) Shi, Y., Gamper, H., and Hearst, J. E. (1987) Interaction of T7 RNA Polymerase with DNA in an Elongation Complex. *J. Biol. Chem.* **263**, 527–534.
(40) Van Houten, B., Gamper, H., Holbrook, S. R., Hearst, J. E., and Sancar, A. (1986) Action Mechanism of ABC Excision Nuclease on a DNA Substrate Containing a Psoralen Crosslink at a Defined Position. *Proc. Natl. Acad. Sci. U.S.A.* **83**, 8077–8081.
(41) Cheng, S., Van Houten, B., Gamper, H. B., Sancar, A., and Hearst, J. E. (1988) Use of Psoralen-Modified Oligonucleotides To Trap Three-Stranded RecA–DNA Complexes and Repair of These Cross-Linked Complexes by ABC Excinuclease. *J. Biol. Chem.* **263**, 15110–15117.